JOURNAL OF SOLID STATE CHEMISTRY 58, 143–152 (1985)

Investigations of Vanadium Oxide Bronzes θ-$(Fe_{1-y}Al_y)_xV_2O_5$

J. J. BARA AND B. F. BOGACZ

Institute of Physics, Jagellonian University, Reymonta 4, 30-065 Cracow, Poland

AND M. PĘKAŁA AND A. POLACZEK

Department of Chemistry, Warsaw University, Al. Żwirki i Wigury 101, 02-089 Warsaw, Poland

Received March 15, 1984; in revised form August 27, 1984

The vanadium oxide bronzes θ-$(Fe_{1-y}Al_y)_xV_2O_5$ are Curie–Weiss paramagnets and hopping semiconductors. The samples studied were synthesized by direct solid-state reaction and investigated by the X-ray diffraction, differential thermal analysis, electrical resistivity, magnetic susceptibility, and Mössbauer techniques. The crystal lattice parameters, effective magnetic moments of Fe^{3+} cations, Curie–Weiss temperatures, and the values of ^{57}Fe hyperfine interaction parameters were determined. Endothermic effects were observed for some of the samples.

Introduction

Previous investigations (*1–3*) of the θ-vanadium oxide bronzes VOB formed with iron and aluminum have shown that these compounds possess properties similar to those of well known β-VOB with the monovalent Li^{1+}, Na^{1+}, K^{1+}, Ag^{1+}, Cu^{1+}, etc., donors (*4, 5*). Both series are Curie–Weiss paramagnets and hopping semiconductors over wide temperature ranges. However, a type of antiferromagnetic interaction (*2, 6, 7*), leading to a spin glass-like phase, observed in θ-$Fe_xV_2O_5$ below 17 K has no analog among other oxide bronzes.

The crystal structure of the θ-VOB was determined by Galy *et al.* (*8*). It is monoclinic, closely related to that of V_6O_{13}. The crystal unit cell contains six formula units ($M_xV_2O_5$). There are $\frac{2}{3}$ holes per formula unit accessible for donor atoms (M). However, not all but only $3x/2$ of them are occupied. It is an open question as to how donor atoms are distributed among crystal sites.

This paper reports the results of investigations performed for the θ-$(Fe_{1-y}Al_y)_xV_2O_5$ VOB by X-ray, differential thermal analysis, electrical resistivity, magnetic susceptibility, and Mössbauer techniques.

As was found earlier (*8*), the homogeneity range ($0.33 \leq x \leq 0.38$) of the θ-FeVOB (θ-$Fe_xV_2O_5$, $y = 0$) is narrower than that ($0.33 \leq x \leq 0.58$) of the θ-AlVOB (θ-$Al_xV_2O_5$, $y = 1$). Thus, not fewer than 50% of holes are occupied in either series and not more than 57 and 88% of holes are occupied in Fe and AlVOB, respectively. The homogeneous solid solutions θ-$(Fe_{1-y}Al_y)_xV_2O_5$ can be easily obtained since the θ-FeVOB are isostructural with θ-AlVOB.

0022-4596/85 $3.00

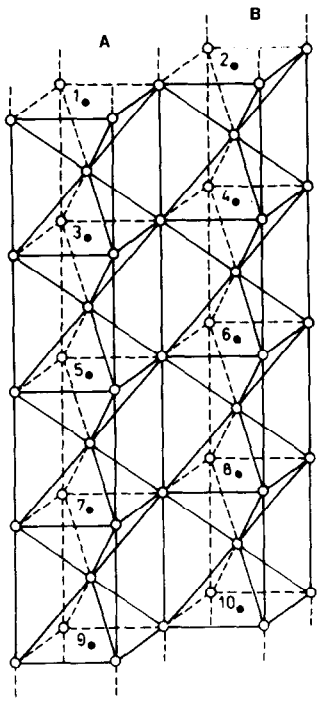

FIG. 1. The tunnels A and B formed by oxygen octahedrons in the crystal structure of the θ phase vanadium oxide bronzes. ○—oxygen atoms, ●—holes accessible for Fe^{3+} or Al^{3+} cations.

Experimental

Two series of θ-$(Fe_{1-y}Al_y)_xV_2O_5$ bronzes were synthesized by a direct solid-state reaction. The first consists of the θ-FeVOB with composition $Fe_xV_2O_5$ ($y = 0$, for $x =$ 0.33, 0.34, 0.35, 0.36, and 0.37). In the second series θ-$(Fe_{1-y}Al_y)_xV_2O_5$ ($x = 0.33$ with $y = 0.00$, 0.152, 0.333, 0.485, 0.667, 0.818, 0.910, and 0.970) iron is partially substituted by aluminum. High-purity V_2O_5 and pulverized iron and aluminum metals were mixed in stoichiometric proportions. For samples with $y = 0.818$, 0.910, and 0.970 the ^{57}Fe isotope was used. The reaction was carried out at 913 K *in vacuo* for 48 hr. The product was thoroughly ground in an agate mortar, pressed into tablets, sealed in evacuated quartz ampoules, repeatedly heated at 893 K for 100 hr, and then left to cool slowly in the oven. The reproducibility of the sample properties was found to be satisfactory. Quenching the sample $(Fe_{0.333}Al_{0.667})_{0.33}V_2O_5$ in its quartz ampoule in cold water had a negligible influence on the Mössbauer absorption spectrum. All the samples were checked for homogeneity by the X-ray diffraction method.

Samples containing only iron ($x = 0.39$, 0.42, and 0.45) exceeding the upper limit of the homogeneity range ($x = 0.38$) were also synthesized and investigated.

The X-ray diffraction studies were performed at room temperature on powdered samples by the Debye–Scherrer method. Some samples were also investigated at 78 K. A Rigaku–Denki X-ray diffractometer was used. The Co-K_α radiation was filtered by a nickel filter.

Differential thermal analysis and thermogravimetry were performed in pure argon atmosphere from room temperature to just above the melting point using a Rigaku–Denki apparatus.

The electrical resistivity measurements were carried out on sintered samples from 20 to 440 K. Four probe dc and ac methods were used. The reproducibility was better than 7%.

Magnetic susceptibility measurements were performed in fields up to 1.6 T over the 78–600 K temperature range by the Faraday method, with electrobalance force recording (*1*). The reproducibility of the results was better than 2%. The susceptibility values were corrected for ionic diamagnetic increments using the data tabulated by Selwood (*9*). It was carefully checked that the measured susceptibility did not depend upon the magnetic field strength.

The ^{57}Fe Mössbauer absorption spectra were recorded at 78, 295, and 423 K. A $^{57}Co(Cr)$ source and the constant acceleration Mössbauer spectrometer of Polon type were used. The velocity scale of Mössbauer absorption spectra was calibrated with a

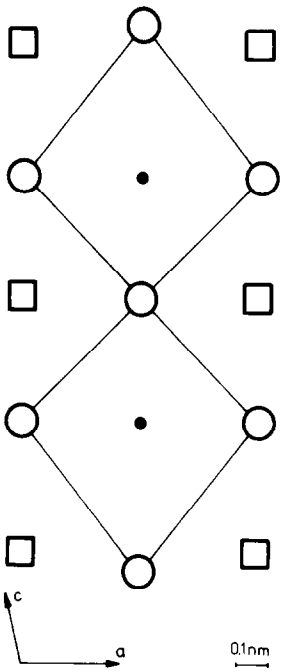

FIG. 2. Nearest neighbors to the lattice holes on the ac plane. ○—oxygen, □—vanadium, ●—holes accessible for Fe^{3+} and Al^{3+} cations.

high-purity metallic iron foil. The Mössbauer absorption spectra were analyzed using a least-squares computer program.

Results and Discussion

The properties of the θ-VOB depend on their crystal structure and distribution of donor atoms (Fe, Al) among accessible crystal sites. Within the crystal lattice of the θ-VOB, one can distinguish double "tunnels" (A, B) formed by oxygen octahedra (Fig. 1). There are $\frac{2}{3}$ holes per formula unit accessible for donor cations. The local charge compensation conditions require that no two adjacent holes along the tunnel remain unoccupied by donor cations. Thus, the x value should not be less than 0.33. This is in accordance with the lower limit of the homogeneity range. For x equal to 0.33 two different types of donor distribution among crystal holes are possible in principle. Both of them, one so-called "zigzag" (1, 4, 5, 8, 9, 12, . . .) type and the other "ladder" (1, 2, 5, 6, 9, 10, . . .) type, lead to ordered crystal structures with unique positions for donor cations in each. Coulomb repulsion should favor the "zigzag" type. For $x > 0.33$ several different surroundings of donor cations are possible. The nearest neighbors of the lattice holes in the ac plane are shown in Fig. 2.

The X-ray diffraction investigations performed at room temperature for θ-$(Fe_{1-y}Al_y)_xV_2O_5$ show very good agreement with the data of Galy *et al.* (*8*). No traces of other phases, other than θ-type were indicated, even for the samples with $y = 0$, $x = 0.39$, 0.42, and 0.45. For the mixed VOB ($y \neq 0$) no broadening of the diffraction peaks was observed, as compared with pure FeVOB ($y = 0$) and pure AlVOB ($y = 1$). The influence of sample composition on the lattice parameters was found to be very small (Table I).

Differential thermal analysis (DTA) was used to detect possible phase transformations within the room temperature–melting point range. The results are shown in Table II. The values of temperatures given in Table II refer to the positions of the peaks on DTA curves recorded during sample heating at constant rate (10 K/min). The DTA

TABLE I

LATTICE PARAMETERS OF VANADIUM OXIDE BRONZES θ-$(Fe_{1-y}Al_y)_xV_2O_5$ DERIVED FROM X-RAY DIFFRACTION DATA

Sample	a [Å] (±0.008)	b [Å] (±0.003)	c [Å] (±0.008)	β [°] (±0.5)
$Al_{0.33}V_2O_5$	12.187	3.672	10.314	103.5
$(Fe_{0.167}Al_{0.833})_{0.33}V_2O_5$	12.183	3.684	10.321	103.0
$(Fe_{0.333}Al_{0.667})_{0.33}V_2O_5$	12.177	3.684	10.316	103.0
$(Fe_{0.500}Al_{0.500})_{0.33}V_2O_5$	12.168	3.684	10.320	103.0
$(Fe_{0.667}Al_{0.333})_{0.33}V_2O_5$	12.163	3.684	10.318	103.0
$(Fe_{0.833}Al_{0.167})_{0.33}V_2O_5$	12.158	3.688	10.321	103.0
$Fe_{0.33}V_2O_5$	12.161	3.692	10.320	102.5
$Fe_{0.35}V_2O_5$	12.160	3.692	10.320	102.5
$Fe_{0.37}V_2O_5$	12.162	3.692	10.322	102.5

TABLE II

DIFFERENTIAL THERMAL ANALYSIS DATA OF VANADIUM OXIDE BRONZES θ-$(Fe_{1-y}Al_y)_xV_2O_5$

Bronze	Melting point (∓2 K)	Other thermal effects observed in the room temperature–melting point range
$(Fe_{0.167}Al_{0.833})_{0.33}V_2O_5$	1003	Inflection point at 368 K
$(Fe_{0.333}Al_{0.667})_{0.33}V_2O_5$	997	Inflection point at 363 K
$(Fe_{0.500}Al_{0.500})_{0.33}V_2O_5$	988	Inflection point at 368 K
$(Fe_{0.667}Al_{0.333})_{0.33}V_2O_5$	985	Endothermic peak at 360 K
$(Fe_{0.833}Al_{0.167})_{0.33}V_2O_5$	983	No effects observed
$Fe_{0.33}V_2O_5$	981	No effects observed
$Fe_{0.35}V_2O_5$	987	No effects observed
$Fe_{0.37}V_2O_5$	982	No effects observed
$Fe_{0.39}V_2O_5$	974	Endothermic peak at 383 K
$Fe_{0.42}V_2O_5$	976	Endothermic peak at 383 K
$Fe_{0.45}V_2O_5$	976	Endothermic peak at 379 K

curves recorded on subsequent cooling of the sample are shifted by no more than 20 K from the corresponding ones toward lower temperature. No changes of the sample during the heating–cooling cycles were detected by the thermogravimetric measurements. It may be seen from Table II that for $0.33 \leq x \leq 0.37$ samples the melting temperature remains practically constant; no thermal effects are observed over the entire range from room temperature to the melting point. For the mixed (Fe–Al)VOB as well as for the samples with $y = 0$, $x = 0.39$, 0.42, and 0.45 endothermic effects were observed at about 363 and 383 K, respectively. The corresponding DTA peaks are of the form, typical for the first-order transitions, but the X-ray diffraction data did not indicate any crystal symmetry changes. Investigations of similar endothermic effects in ^{57}Fe-doped θ-AlVOB are in progress (*10*).

The magnetic susceptibility measurements performed in the temperature range from 78 to 600 K, showed that the bronzes θ-$(Fe_{1-y}Al_y)_xV_2O_5$ are Curie–Weiss paramagnets. There are two types of paramagnetic cations V^{4+} ($3d^1$) and Fe^{3+} ($3d^5$) in each sample. They originate from transfer of valence electrons from donor atoms (Fe, Al) to vanadium atoms (*4*, *5*) according to the scheme

$$M_{\text{metal}} + 3V^{5+}_{\text{oxide}} \rightarrow (M^{3+} + 3V^{4+})_{\text{bronze}}.$$

The existence of one sort of paramagnetic vanadium cations (V^{4+}) in pure θ-AlVOB ($y = 1$) and additionally, of one sort of paramagnetic iron cations (Fe^{3+}) in pure θ-FeVOB ($y = 0$) was already established (*2*, *11*, *12*) by ESR and Mössbauer methods, respectively. For the θ-AlVOB, of not too large x values, for which the signal broadening is not too great, a single and nearly symmetrical ESR signal with $g = 1.97$ was always observed at room temperature. The previous (*11*, *12*) and present Mössbauer effect data of θ-VOB indicate the existence of iron atoms in the high-spin Fe^{3+} ($^6S_{5/2}$) state.

It is assumed (*1*, *4*, *5*) that both Fe^{3+} and V^{4+} paramagnetic subsystems additively contribute to the temperature-dependent magnetic susceptibility of θ-$(Fe_{1-y}Al_y)_xV_2O_5$ according to

$$\chi_{\text{bronze}} = C_{\text{Fe}}(T - \theta_{\text{Fe}})^{-1} + C_{\text{V}}(T - \theta_{\text{V}})^{-1}, \quad (1)$$

where T is temperature, while C and θ are the Curie constant and Weiss parameter, respectively, for Fe and V subsystems. In this approximation, the vanadium contribution to the total magnetic susceptibility of pure FeVOB has the same value as the magnetic susceptibility of isostoichiometric pure AlVOB in which only one type (V^{4+}) of paramagnetic cations exists. Therefore, the iron contribution to the total magnetic susceptibility of pure FeVOB can be determined by subtracting the vanadium contribution from the total magnetic susceptibility. The value of vanadium contribution is known from measurements performed for θ-AlVOB. In this approximation we have

TABLE III

VALUES OF THE EFFECTIVE MAGNETIC MOMENT p_{eff}(Fe) AND THE WEISS PARAMETER θ_{Fe} DETERMINED FROM THE MAGNETIC SUSCEPTIBILITY MEASUREMENTS OF VANADIUM OXIDE BRONZES θ-$(Fe_{1-y}Al_y)_xV_2O_5$ PERFORMED IN THE RANGE 78–600 K

Bronze	p_{eff} [μ_B]	θ_{Fe} [K]
$(Fe_{0.333}Al_{0.667})_{0.33}V_2O_5$	5.55	−52
$(Fe_{0.500}Al_{0.500})_{0.33}V_2O_5$	5.50	−60
$(Fe_{0.667}Al_{0.333})_{0.33}V_2O_5$	5.40	−61
$(Fe_{0.833}Al_{0.167})_{0.33}V_2O_5$	5.40	−70
$Fe_{0.33}V_2O_5$	5.28	−81
$Fe_{0.35}V_2O_5$	5.31	−115
$Fe_{0.37}V_2O_5$	5.39	−105

$$\chi_{Fe} = \chi_{tot}(Fe_xV_2O_5) - \chi_{tot}(Al_xV_2O_5) = C_{Fe}(T - \theta_{Fe})^{-1}, \quad (2)$$

where $C_{Fe} = N_{Fe}p_{eff}^2(Fe)\mu_B^2/3k_B$, N_{Fe} is the number of Fe^{3+} cations per cubic centimeter, $p_{eff}(Fe)$ is the effective magnetic moment of Fe^{3+} cation, μ_B is the Bohr magneton, while k_B is the Boltzmann constant.

The method described above was used to determine the $p_{eff}(Fe)$ and θ values for the θ-$(Fe_{1-y}Al_y)_xV_2O_5$. The results so obtained are collected in Table III. It should be stressed that the values of $p_{eff}(Fe)$ given in Table III are determined for the trivalent iron state. This assumption is based on our ^{57}Fe Mössbauer effect data and on the crystallochemical considerations regarding the isostructurality of θ-FeVOB and θ-AlVOB. It is noteworthy that the $p_{eff}(Fe)$ values for θ-$(Fe_{1-y}Al_y)_xV_2O_5$ are considerably lower than both the theoretical and experimental values usually found for compounds with trivalent high-spin state iron. The reduction of the p_{eff} for the $Fe^{3+}(^6S_{5/2})$ ions as compared with the theoretical value was observed for some Fe–V–O systems by Pebler *et al.* (*13*) and by Atzmony *et al.* (*14*). According to Pebler this reduction is due to Fe^{3+}–V^{4+} near-neighbor interaction. This may also be true for the θ-$(Fe_{1-y}Al_y)_xV_2O_5$ system. The large value of the isotropic ^{51}V NMR shift observed for θ-FeVOB (*15*) may support this hypothesis.

The electrical resistivity measurements were performed only on sintered polycrystalline samples of VOB. The temperature dependence of the electrical resistivity shown in Fig. 3 for $Al_{0.33}V_2O_5$ and $Fe_{0.33}V_2O_5$ is typical for all bronzes investigated. It is seen that in each case, in the range 20–300 K, the type of the donor atoms, Al or Fe, does not influence the magnitude of resistivity. Thus, the donor atomic orbitals play, if any, only a minor role in the electron transport processes. This indicates that the donor valence electrons are completely transferred to the oxide matrix states in accordance with Sienko's model (*4*).

The θ-VOB behave like semiconductors and become very highly resistive (10^9 Ω cm) below about 20 K. It is assumed that the electrical transport in θ-VOB proceeds via hopping of the electrons between the adjacent vanadium sites (*16*):

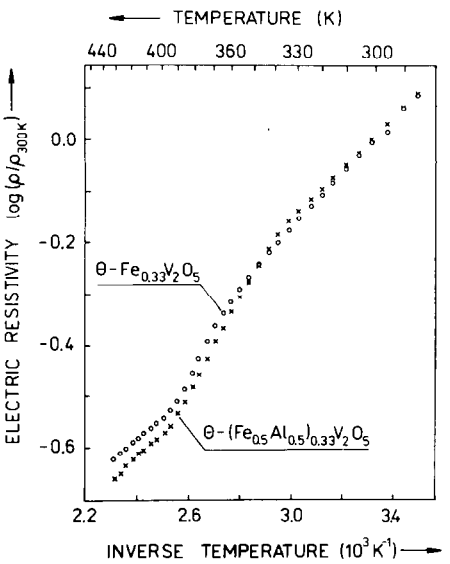

FIG. 3. The typical temperature dependence of the relative electrical resistivity of $Fe_{0.33}V_2O_5$ and $(Fe_{0.500}Al_{0.500})_{0.33}V_2O_5$.

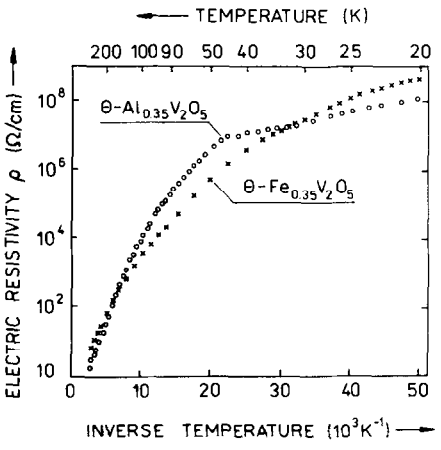

FIG. 4. The temperature dependence of the electrical resistivity of $Al_{0.35}V_2O_5$ and $Fe_{0.35}V_2O_5$.

$$V^{4+}(V^{5+})_{\text{site A}} \overset{e^-}{\leftrightarrow} V^{5+}(V^{4+})_{\text{site B}}.$$

This mechanism of the conduction seems to be well proven for the case of the β-VOB (*5*), which, with regard to their electrical properties, have much in common with the θ-VOB.

The electrical resistivity measurements were also made above room temperature in order to study the resistivity behavior in the vicinity of anomalies observed in the magnetic susceptibility and DTA. As was reported recently (*3*), the magnetic susceptibility as well as the effective magnetic moment per V^{4+} ion increase abruptly in θ-AlVOB above $T_k \approx 345$ K. A similar effect could not be observed either in pure or in mixed iron containing VOB which may be due in part to the overwhelming iron contribution to the total susceptibility. The typical temperature dependence of the relative resistivity (normalized to the ρ(300 K) value) is shown in Fig. 4. It may be seen that two semiconducting temperature intervals are separated by the transition temperature range. The transition temperature range is narrow and close to $T_k \approx 380$ K in the pure FeVOB, while it is broadened and shifted toward lower temperature as the Al content increases, to a value of ≈345 K for $(Fe_{0.50}Al_{0.50})_{0.33}V_2O_5$. The surprising lack of any endothermic effect about $T_k \approx 380$ K in DTA measurements on pure FeVOB (see Table II) suggests that, compared to resistivity measurements, this effect is smeared out over a broad temperature interval and/or is very weakly pronounced in the DTA curve.

In order to obtain some microscopic insight into the properties of the investigated VOB, the Mössbauer spectroscopy was used, as it can distinguish not only nonequivalent electronic states and nonequiva-

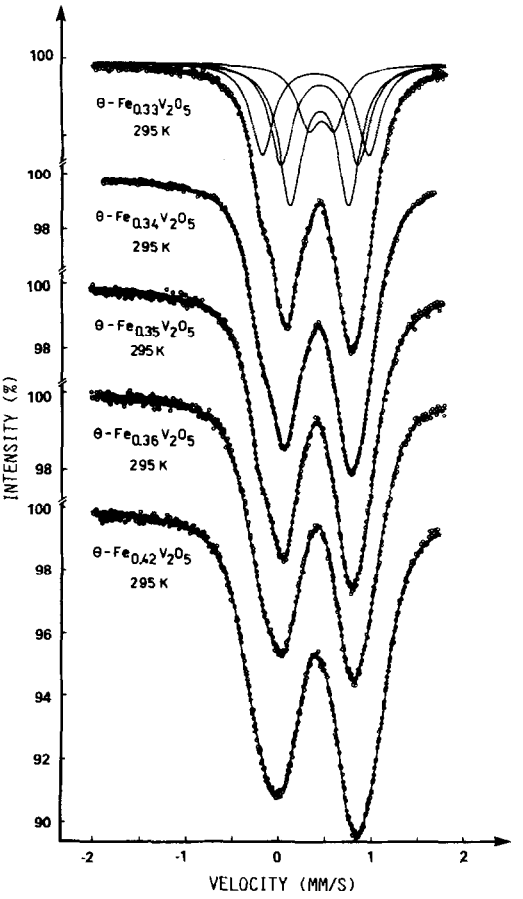

FIG. 5. The typical ^{57}Fe Mössbauer spectra recorded at room temperature for selected samples of pure FeVOB. The spectra were resolved into four symmetric quadrupole doublets.

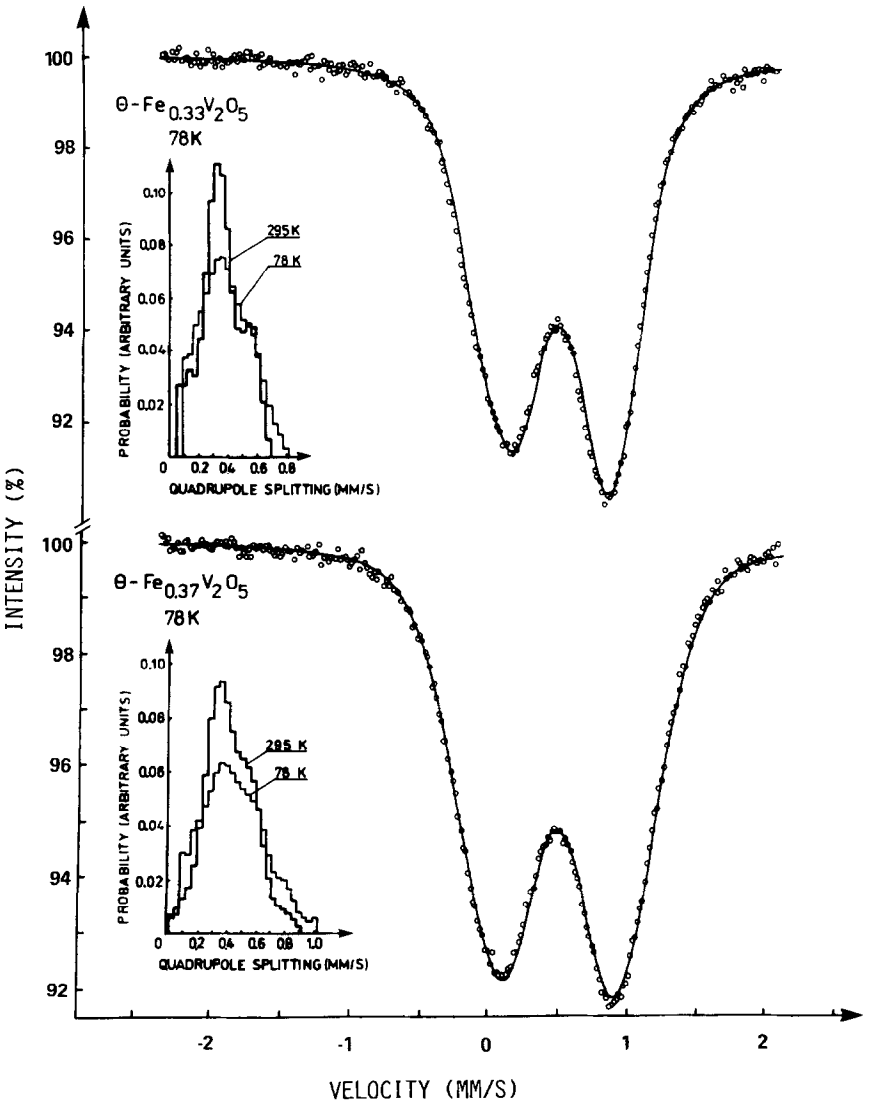

FIG. 6. The ^{57}Fe Mössbauer absorption spectra recorded at 78 K for θ-$Fe_{0.33}V_2O_5$ and θ-$Fe_{0.37}V_2O_5$ with the corresponding quadrupole splitting diagrams. The room-temperature diagrams are inserted for comparison.

lent crystal sites of the resonant isotope but, also nonequivalent near-neighbor configurations of a given type of crystal site. Considerable effort was put in on the numerical analysis of the Mössbauer absorption spectra. The Mössbauer absorption spectra (Figs. 5–7) are of the form of broad asymmetric doublets. Since not all of the accessible lattice sites are occupied by Fe(Al) atoms, a statistical distribution of Fe(Al) atoms was assumed in first approximation, and the distribution of quadrupole splittings (Fig. 6) was calculated from the absorption spectra. The field distribution computer procedure, described in Refs. (*17, 18*) was used for this purpose. Poorly resolved maxima were observed in some of the quadrupole splitting distribution dia-

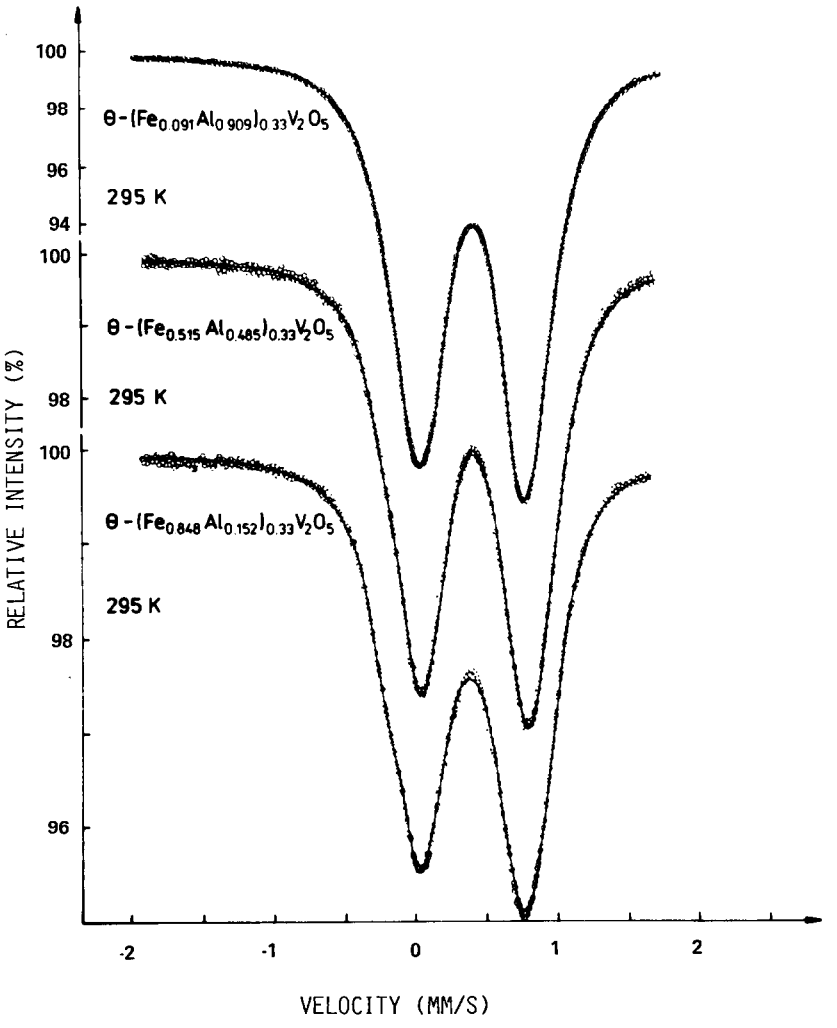

FIG. 7. The ^{57}Fe Mössbauer absorption spectra recorded at room temperature for selected samples of the θ-$(Fe_{1-y}Al_y)_xV_2O_5$ oxide bronzes. Spectra were resolved into four symmetric quadrupole doublets.

grams. They suggest the existence of a few sets of nonequivalent surroundings to the lattice sites occupied by resonant isotope. Thus, in the next step of computation, discrete values of quadrupole splittings were assumed. After some trials, it was found that each of Mössbauer absorption spectra can be well decomposed into four symmetric quadrupole doublets with equal linewidths (Figs. 5 and 7). The correctness of such a decomposition was established by χ^2 tests. The hyperfine interaction parameters derived from the Mössbauer absorption spectra are shown in Fig. 8, where the Duncan–Golding boundaries (*19*) of the Fe^{3+} high-spin compounds are marked.

The isomer shift and quadrupole splitting data prove that iron atoms in θ-$(Fe_{1-y}Al_y)_xV_2O_5$ are in the $Fe^{3+}(^6S_{5/2})$ state. This observation supports the hypothesis

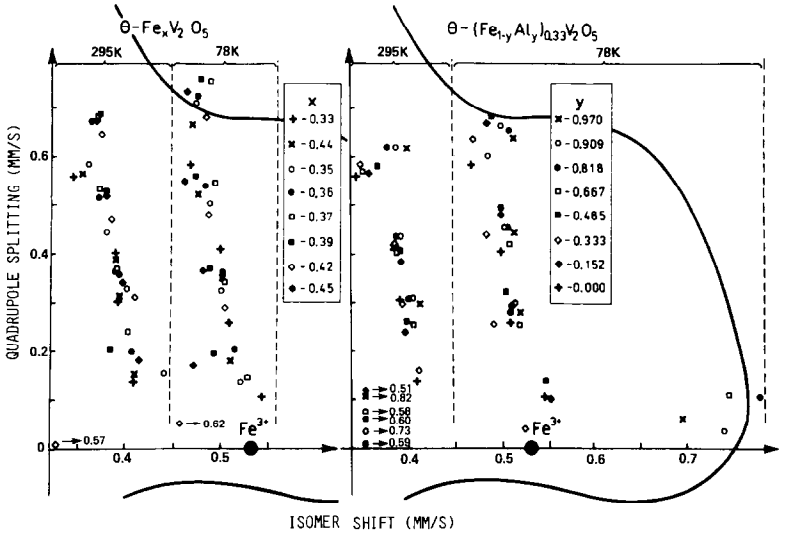

FIG. 8. The correlation between the room-temperature isomer shift and quadrupole splitting values of investigated vanadium oxide bronzes. The Duncan–Golding boundaries of the Fe^{3+} high-spin compounds (*19*) are marked with a solid line. The liquid-nitrogen temperature data are inserted for comparison. The number written near the arrow indicates the value of isomer shift to which the point should be shifted.

according to which the valence electron of donor Fe atoms are transferred to vanadium atoms (*4*). The isomer shift values are at most only slightly influenced by sample composition. The quadrupole splittings of all doublets of θ-$(Fe_xV_2O_5$ ($y = 0$) series slightly increase of Fe concentration. For the θ-$(Fe_{1-y}Al_y)_xV_2O_5$ ($y \neq 0$) series no such correlation is observed. In general, the relative contributions of individual quadrupole doublets to the total resonance absorption of θ-$(Fe_{1-y}Al_y)_xV_2O_5$ ($0 \leq y < 1$) series are not temperature dependent, although some of them are slightly influenced by the composition of the sample. The hyperfine interaction parameters of θ-$(Fe_{1-y}Al_y)_xV_2O_5$ ($0 < y < 1$) series do not indicate any pronounced influence of Al on the Mössbauer absorption spectra. However, the scatter of the hyperfine interaction parameters of this series, which is larger than that of pure FeVOB, may be due to presence of Al atoms.

Thus far, we have not succeeded in assigning the observed quadrupole doublets to the four nonequivalent types of surroundings of lattice positions occupied by Fe atoms. Most likely both the distribution of Fe^{3+} cations among the accessible lattice sites and distributions of V^{4+} and V^{5+} nearest neighbors of Fe^{3+} cation contribute some number of nonequivalent surroundings of Fe^{+} cations.

In contrast to ^{57}Fe-doped θ-AlVOB (*10*), the endothermic effects indicated by the DTA method for some of the investigated samples (Table II) were not detected by the Mössbauer effect method.

Although we have applied several complementary methods in studies of the θ-$(Fe_{1-y}Al_y)_xV_2O_5$ and have obtained valuable information on their crystal, magnetic, and electrical properties, there are still some open questions to be answered. Investigations of endothermic effects, observed in ^{57}Fe-doped AlVOB, are in progress.

References

1. M. PĘKAŁA AND A. POLACZEK, *Pol. J. Chem.* **52,** 353 (1978).
2. M. PĘKAŁA AND A. POLACZEK, *Phys. Status Solidi A* **58,** 533 (1980).
3. M. PĘKAŁA AND A. POLACZEK, *Acta Phys. Pol. A* **63,** 339 (1983).
4. M. J. SIENKO, *Adv. Chem. Ser.* **39,** 224 (1963); *Alkali Met.* **22,** 429 (1967).
5. J. H. PERLSTEIN AND M. J. SIENKO, *J. Chem. Phys.* **48,** 174 (1968); H. KESSLER AND M. J. SIENKO, *J. Solid State Chem.* **1,** 152 (1970).
6. M. PĘKAŁA AND A. POLACZEK, *Solid State Commun.* **34,** 275 (1980).
7. M. PĘKALA AND A. POLACZEK, *J. Magn. Magn. Mater.* **21,** 196 (1980).
8. J. GALY, A. CASALOT, J. DARRIET, AND P. HAGENMULLER, *Bull. Soc. Chim. Fr.* **1,** 227 (1967); J. GALY, M. POUCHARD, A. CASALOT, AND P. HAGENMULLER, *Bull. Soc. Fr. Mineral. Cristallogr.* **90,** 544 (1967); P. HAGENMULLER, J. GALY, M. POUCHARD, AND A. CASALOT, *Mater. Res. Bull.* **1,** 95 (1966).
9. P. W. SELWOOD, "Magnetochemistry," Interscience, New York 1956.
10. J. J. BARA, B. F. BOGACZ, M. PĘKAŁA, AND A. POLACZEK, to be published.
11. J. KORECKI, A. POLACZEK, AND M. PĘKAŁA, *Nucl. Instrum. Methods* **199,** 209 (1982).
12. M. BARAN AND A. POLACZEK, *Phys. Status Solidi A* **25,** K13 (1974).
13. J. PEBLER, K. SCHMIDT, AND G. WEISER, *Phys. Status Solidi A* **56,** 457 (1979); J. PEBLER AND K. SCHMIDT, *Phys. Status Solidi A* **56,** 279 (1979).
14. U. ATZMONY, E. GUREWITZ, M. MELAMUD, H. PINTO, H. SHAKED, G. GORODETSKY, E. HERMON, R. M. HORNREICH, S. SHTRIKMAN, AND B. WANKLYN, *Phys. Rev. Lett.* **43,** 782 (1979).
15. R. N. PLETNEV, V. L. VOLKOV, M. PĘKAŁA, AND A. POLACZEK, *Phys. Status Solidi A* **58,** K17 (1980).
16. S. KRUPIĆKA, "Fizika Ferritov," Vol. 2, p. 422, Mir Publ., Moscow (1976).
17. H. HESSE AND A. RÜBARTSCH, *J. Phys. E* **7,** 526 (1974).
18. G. LECAER AND J. M. DUBOIS, *J. Phys. E* **12,** 1083 (1979).
19. J. F. DUNCAN AND R. M. GOLDING, *Quart. Rev.* **19,** 36 (1966).